E-Infrastructures

H2020-EINFRA-2015-1

EINFRA-5-2015: Centres of Excellence for computing applications

EoCoE

Energy oriented Center of Excellence

for computing applications

Grant Agreement Number: EINFRA-676629

D4.3 - M35

Layout of an energy supply system for Teveren based on geothermal direct-heat.

Project and Deliverable Information Sheet

EoCoE	Project Ref:	EINFRA-676629
	Project Title:	Energy oriented Centre of Excellence
	Project Web Site:	http://www.eocoe.eu
	Deliverable ID:	D4.3
	Lead Beneficiary:	RWTH & Juelich
	Contact:	Jan Niederau
	Contact's e-mail:	jniederau@eonerc.rwth-aachen.de
	Deliverable Nature:	Report
	Dissemination Level:	PU*
	Contractual Date of Delivery:	M35 31/08/2018
	Actual Date of Delivery:	M30 20/04/2018
	EC Project Officer:	Carlos Morais-Pires

* - The dissemination level are indicated as follows: PU – Public, CO – Confidential, only for members of the consortium (including the Commission Services) CL – Classified, as referred to in Commission Decision 2991/844/EC.

Document Control Sheet

Document	Title :	Layout of an energy supply system for Teveren based on geothermal direct-heat.
	ID :	D4.3
	Available at:	http://www.eocoe.eu
	Software tool:	LaTeX
Authorship	Written by:	Jan Niederau
	Contributors:	Alexander Michalski, Henrik Büesing, Johanna Bruckmann
	Reviewed by:	Nathalie Girard, Edouard Audit, PEC members

Contents

List of Figures

List of Tables

1. Introduction

Deliverable 4.3 is the continuation of work done in Task 4.1 (*Geothermal energy HPSC issues*, described in Deliverable report 4.2). It summarizes the work done in the consecutive Task 4.2, which is the simulation and assessment of geothermal energy supply based on findings of Task 4.1. Simulation results of the posterior ensemble presented in Deliverable 4.2 pose the initial conditions for transient simulations of different Borehole Heat Exchanger (abbreviation BHE) layouts (fourth step in Fig. 1), which are simulated for assessing the possibility of geothermal direct heat supply in the target area, especially by considering retrofit of buildings.

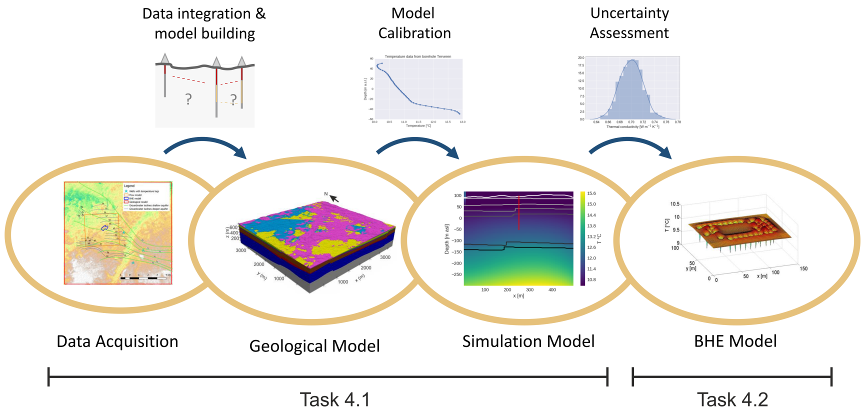

Figure 1: Conceptual workflow of Task 4.1 and Task 4.2. Deliverable 4.3 comprises the fourth step, i.e. Task 4.2. The input parameters are a direct result of step one to three, i.e. content of Task 4.1.

To this end, we simulated the total heating power demand for representative buildings in the settlement, using the software TEASER Remmen et al. (2018). The specific heating power demands were used as operating parameters for borehole heat exchanger fields simulated with SHEMAT-Suite. In the following, this report will cover the selection process of representative Buildings in the target area, the assessment of corresponding heating power demands, and the implementation of a BHE-field based on this selection. Simulations of Borehole Heat Exchangers (BHE) were done in a two-step process, where we first simulated a BHE explicitly, secondly implemented a field consisting of multiple BHE.

2. BHE Simulation layout

Several layouts for BHE fields were tested during Task 4.2, considering different development scenarios for the studied settlement. This settlement *"Fliegerhorstsiedlung Teveren"* (further called Neuteveren) near Geilenkirchen, is a former military housing complex adjacent to the NATO-Airbase Geilenkirchen. The buildings in the settlement (built in the 1950s) are planned to be extensively retrofitted, in addition to new houses planned for construction. Figure 2 shows a map showing the location of Neuteveren (blue polygon) within the flow model of Deliverable 4.2 (turquoise polygon in cut-out). Small grey rectangles depict positions of existing houses, further colors the surface geology. Two representative locations for modelling BHE-fields were chosen based on information available in a confidential planning report provided by representatives of the city of Geilenkirchten.

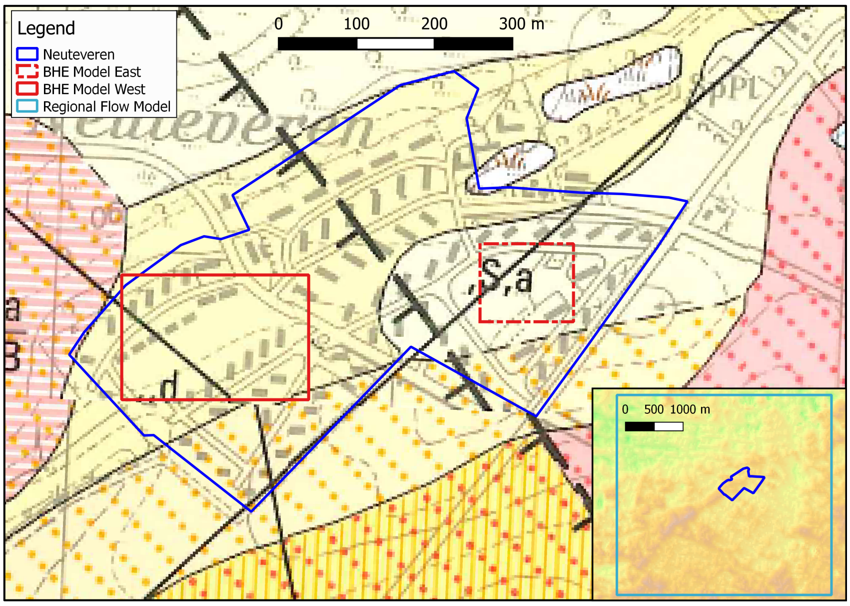

Figure 2: Geological map of the Settlement Neuteveren. The blue polygon outlines the settlement, with grey rectangles representing existing buildings. Two representative BHE-Models (red squares) were created for modelling the transient characteristics of potentially installed borehole heat exchangers.

Parameters considered were, among others, available building refitting parameters (building area, date of construction, floors), advantegeous location for probable investors. Those parameters were combined with results of Deliverable 4.2 for deciding on model locations for BHE-fields. The western model part (solid red square in Fig. 2) are houses, which will be refitted. In the eastern part of the area (dashed red square in Fig. 2) new single-family houses, or semi-detached houses may be built, according to information provided by city representatives. For the western part, we simulated a BHE-field for original and refitted conditions. In the chosen layout, one borehole heat exchanger is assumed to be installed

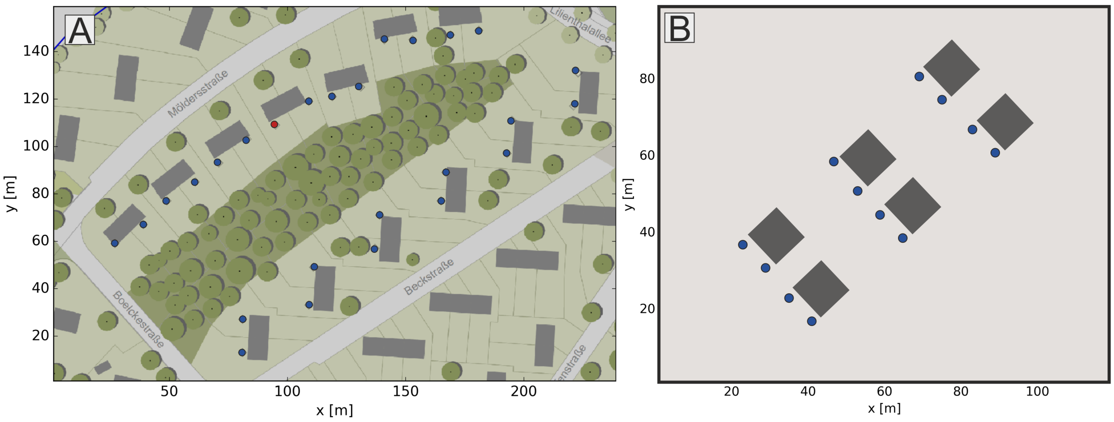

Figure 3: Positions of borehole heat exchangers (blue circles) in the numerical models (A: western model, B: eastern model). Each borehole heat exchanger is assigned to a housing unit. The red circle marks the BHE picked for exemplarily presenting the transient temperature development in a BHE.

per housing unit, yielding 26 BHEs in the western model (Fig. 3, A), and 6 to 12 in the eastern model, depending on the planned construction scenario (Fig. 3, B). Exact position and layout of new buildings is yet confidential. Thus the map of the eastern model is simplified, as the buildings shown in Figure 3 B represent one possible scenario to be realized. Further existing development scenarios (Geilenkirchen, 2018) differ in layout of newly built houses. However, due to the relative continuous geology in the subsurface of Teveren, simulation results of one scenario are generally representative for BHE operation in the area. All BHE units extend to a depth of 100 m below ground surface. This is a regular depth for geothermal borehole heat exchangers, as depths greater than 100 m require more extensive reviews based on the german mining law.

3. Explicite Borehole Heat Exchanger

In order to assess the direct response of the subsurface to an installed borehole heat exchanger, we simulate a borehole heat exchanger unit explicitely. That is, the model resolves the BHE design, i.e. materials and geometries within a borehole. Such designs

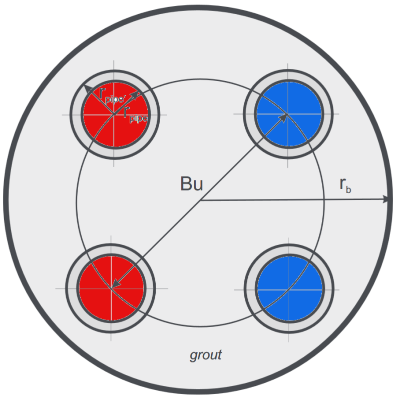

Figure 4: Cross-section of a double-U shaped BHE with indicated geometries. Pipes are colored according to upflow (red) or downflow (blue) (modified from Mottaghy & Dijkshoorn (2012)).

are e.g. coaxial BHE or double U-shaped BHE, the latter being implemented in our model. For this, we follow the approach presented in Mottaghy & Dijkshoorn (2012), which is based on assessing heat flow rates between BHE pipes (see Fig. 4) $\dot{Q}_e$, and the heat flow rate from the surrounding rocks $\dot{Q}_r$:

$$\dot{Q}_e = \frac{0.5((T_d^{t-1}(i+1) + T_d^{t-1}(i)) - (T_u^{t-1}(i+1) + T_u^{t-1}(i)))}{R_a} \tag{1}$$

$$\dot{Q}_r = \frac{T_r^{t-1} - 0.5(T_d^{t-1}(i+1) + T_d^{t-1}(i))}{R_b} \tag{2}$$

where T_u and T_d are temperatures in the upflow and downflow pipes, respectively. Explicite time stepping is used, as indicated by the superscript $(t-1)$. The spatial location along the BHE is defined by the index (i). R_a and R_b are the internal thermal resistance (between pipes) and total borehole thermal resistance respectively. For an extensive derivation of these thermal resistances, see Hellström (1991). Geometric parameters specified in Figure 4 are coupled to SHEMAT-Suite (Clauser, 2003; Rath et al., 2006) by a parameter file. Within SHEMAT-Suite, a BHE is introduced as an effective heat generation term (positive for surface cooling applications, negative for surface heating applications) which directly correlates to the heat flow rate $\dot{Q}_r$. For testing the temperature response of a BHE installation, we prescribe the inlet temperature (i.e. temperature at downflow pipes in Fig. 4) and pumping rate as a time series of real data taken from the BHE-field of the E.ON

ERC Building (Bode et al., 2018) over a timeframe of 3 days. Figure 5 shows the prescribed

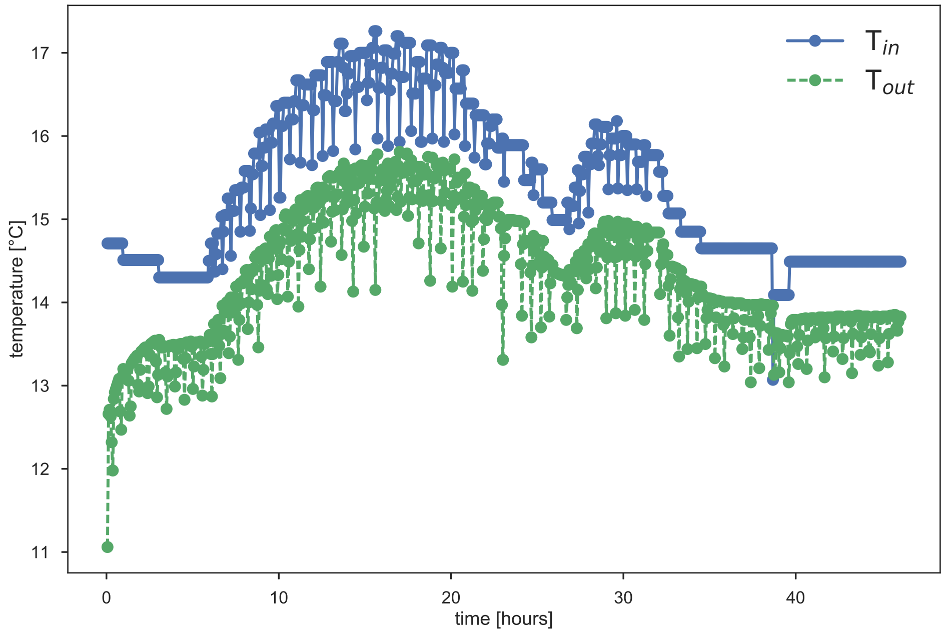

Figure 5: Transient temperature development of inlet temperature (blue) and outlet temperature (green) in the explicite BHE model over a time period of three days during a cooling cycle. Relatively low temperatures of T_{out} at the beginning of the simulation are due the initial temperature conditions.

inlet temperature T_{in} and the outlet temperature T_{out} of the BHE, which is calculated by SHEMAT-Suite. Horizontal lines at the inlet temperature over longer timescales represent no change in energy demand, i.e. no acitivity. Overall, outlet temperature shows a good and fast response to the prescribed inlet temperatures. At the beginning of the simulation, T_{out} is equal to the undisturbed subsurface temperature, thus significantly lower compared to later outlet temperatures. Potential available thermal power directly depends on the difference between T_{in} and T_{out}. In order to assess the sustainability of BHE installations, longer timescales need to be simulated. However, the explicite test over a short time scale already suggests, that the model provides reasonable results, as outlet temperatures correctly respond to inlet temperatures, which in turn reflect the cooling power demand.

4. Thermal energy demand

In order to estimate the sustainability of a geothermal direct heat usage via BHEs, knowledge about the transient thermal energy demand of residential buildings is essential. We use TEASER (**T**ool for **E**nergy **A**nalysis and **S**imulation for **E**fficient **R**etrofit) (Remmen et al., 2018) for generating times series containing the heating power demand for the specified number of residential buildings. TEASER uses Reduced Order Models (ROMs) whose input parameters are defined by the user and data enrichment functions. By using those functions, the necessary user-input is reduced to a minimum, summarised in table 1. The thermal energy demand of a building is a function of the outdoor temperature. Unless specified differently, TEASER uses a representative annual temperature curve as a data enrichment function. For the thermal energy demand of buildings in the models presented here, we specify the local annual outdoor temperature curve of 2014 as additional input parameter (Fig. 6 top). Using annual temperature curves and building parameters

Table 1: Building parameters used as simulation input for TEASER.

Building parameter	Value	Unit
Building usage type	Residential	-
Year of construction	1953 (original)	-
	2016 (refitted)	-
Number of floors	2	-
Floor height	2.8	m
Net lease area	104 (west)	m^2
	158 (east)	m^2

as input, TEASER creates building models, which in turn are used as input for other simulation codes, modelling the thermal energy demand of buildings. The bottom plots in Figure 6 show the thermal power demand of buildings over a year for the western model (Fig. 6 mid) and the eastern model (Fig. 6 bottom). In the western model, we generated thermal power demand curves for buildings in original (blue) and refitted state (green). Energy efficiency of refitted buildings compared to older buildings is clearly visible in winter months, whereas differences are smaller during summer months. Thermal energy demand for old buildings is more volatile, due to less thermal insulation compared to refitted buildings. Note that thermal energy demand is cut at 0 kW, as just heating energy demand is taken into account. If cooling in summer should be considered, thermal energy demand can also get negativ, indicating heat storage in the subsurface.

5. Model parameters

As previously mentioned, two models were generated for assessing BHE performance in Teveren. The models are discretized in a equidistant hexahedral grid with a cell size of 2 m × 2 m × 5 m (x × y × z). Six geological units are resolved in this model, with the Inden Layers being the deepest and the Quaternary Aquifer being the shallowest unit. Their main petrophysical properties and values are listed in table 2. In Task 4.1, these property values (thermal conductivity and porosity) were determined by a gradient based inversion. Average permeability was determined by a MonteCarlo approach. The MonteCarlo ensemble was conditioned using groundwater table data (called apos-

Table 2: Geological units and ascribed petrophysical properties used for the BHE Models. The properties are result of the inversion described in D4.2. Units are ordered how they would be encountered in a borehole, i.e. from shallowest (Quaternary Aquifer) to deepest (Inden Layers).

Model Unit	Porosity	vertical Permeability (m^2)	Thermal Conductivity (matrix; $W\,m^{-1}\,K^{-1}$)
Quaternary Aquifer	0.203	$1.01\,10^{-10}$	2.34
Upper Rotton	0.33	$3.7\,10^{-16}$	1.88
Hauptkies Aquifer	0.239	$1.19\,10^{-10}$	2.63
Seam Schophoven	0.303	$2.5\,10^{-16}$	0.95
Inden Layers & Ville Layers	0.193 & 0.205	$1.\,10^{-13}$	2.78 & 2.3

teriori ensemble), yielding conditioned probabilities for permeability values of each unit. In addition to permeability values, initial- and boundary conditions for the BHE models result directly from the aposteriori ensemble described in Deliverable 4.2. The flow model

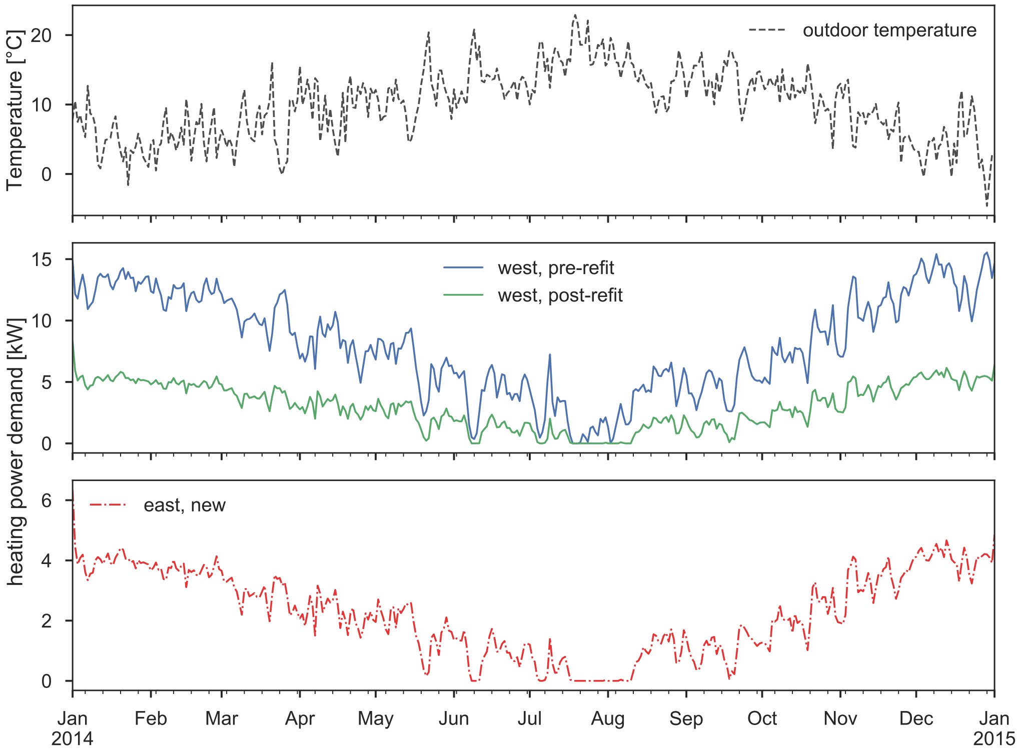

Figure 6: Top: measured air temperature in 2014. Mid: heating power demand of a twin-house in the western model. Bottom: heating power demand of a one-family house in the eastern model

described in D4.2 is significantly larger than the BHE models. Values for temperature and hydraulic head were cut from the flow model according to the boundaries of each single BHE model, interpolated to the finer grid of the BHE models, and set as initial- and boundary conditions. That is, we apply dirichlet boundary conditions for hydraulic head and temperature to the lateral boundaries. Figure 7 shows the initial groundwater levels (in m a.s.l.) in the BHE models. These values are used for initial and boundary condition values of the hydraulic potential (hydraulic head). The general gradient in hydraulic potential is from south to north, implying an according northward groundwater flow. This agrees with coarse groundwater level data (Erftverband, 2015). For evaluating the interaction of BHEs, knowledge of the natural groundwater flow direction and velocity is essential. The explicite formulation for BHE described in section 3 turned out to be too time consuming for simulating whole BHE-fields, as it requires small time steps to satisfy the Courant criterion (Mottaghy & Dijkshoorn, 2012). For simulating a field of several BHEs, we use an approximation described in Mottaghy & Dijkshoorn (2012), where power demand is translated into an effective heat source term, heat sink term respectively, along the BHE. This enables a more efficient simulation of larger BHE-fields, e.g. the western model which comprises 26 BHEs. For calculating the necessary heat source or sink term along a BHE, the total power demand has to be known. SHEMAT-Suite evenly apportions the total power demand among the available BHE units. As buildings in each of our BHE models have the same design and approximate net-lease area, we can assume that each building equally contributes to the total heating- or cooling demand. In order to assess the total heating power demand, we multiply the transient demand (Fig. 6, mid and bottom) with the number of buildings to be supplied with geothermal heat. That is,

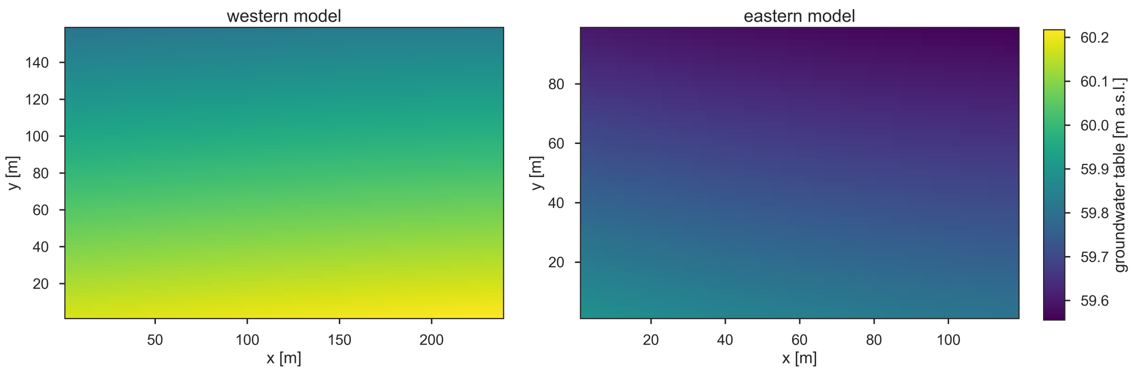

Figure 7: Map view of hydraulic potential in the western model (left) and the eastern model (right). Values of hydraulic head at lateral boundaries are kept constant and work as boundary conditions.

for the western model, we multiply the heating power demand by 13 (26 houses arranged as 13 twin-houses), as the demand is calculated for a whole twin-house.

6. Results

Operation of the BHE-fields in the western, as well as in the eastern model, was simulated over the timeframe of one year in order to assess the impact of seasonal heating demand and groundwater flow on the BHE-field. Simulation results of the western and eastern model are presented as 2D snapshots, i.e. horizontal cross-sections at a depth of 50 m below surface. For the western model, we additionally analyze the temperature variation in one representative BHE a time series.

6.1 Western model simulation

We designed the western BHE-field model around existing buildings which are representative for the settlement Teveren. Already existing buildings provide the possibility for assessing the impact of refitting buildings on the BHE-field. As such, we generated two scenarios for the western model. One using an estimated heating power demand of the buildings in original state (Fig. 6, middle, blue curve) and a scenario which assumes refit of buildings based on newest energy standards (Fig. 6 middle, green curve). Figure 8 shows temperature at a depth of 50 m below ground surface assuming refitted buildings (left) or buildings in original state (right). The latter have a significantly higher heating power demand due to less heat insulation. This in turn causes lower temperatures in the BHEs compared to energetically renovated buildings. Temperatures around BHEs in the original scenario are around 2 °C lower than in the renovated scenario.
Depending on aquifer permeability, groundwater flow shows a significant impact on temperatures around the BHE-field, as plumes of relatively lower temperatures are transported northward along the local groundwater flow direction. As heating power demand for buildings in the original scenario is higher, the thermal plumes are more pronounced. Consequently, the interaction between single heat exchangers is stronger, as BHEs in northern part of the model are affected by thermal plumes coming from neighbouring installations. Further, simulations suggest that aligning BHEs in a north-south direction is not advantageous, as this is parallel to the direction of propagation of thermal plumes (see southern pairs of BHEs in Fig. 8). For assessing how much a transported thermal plume affects neighbouring borehole heat exchangers, we study the temperature development over time of two BHEs in the southern part of the model. Temperature differences between neigh-

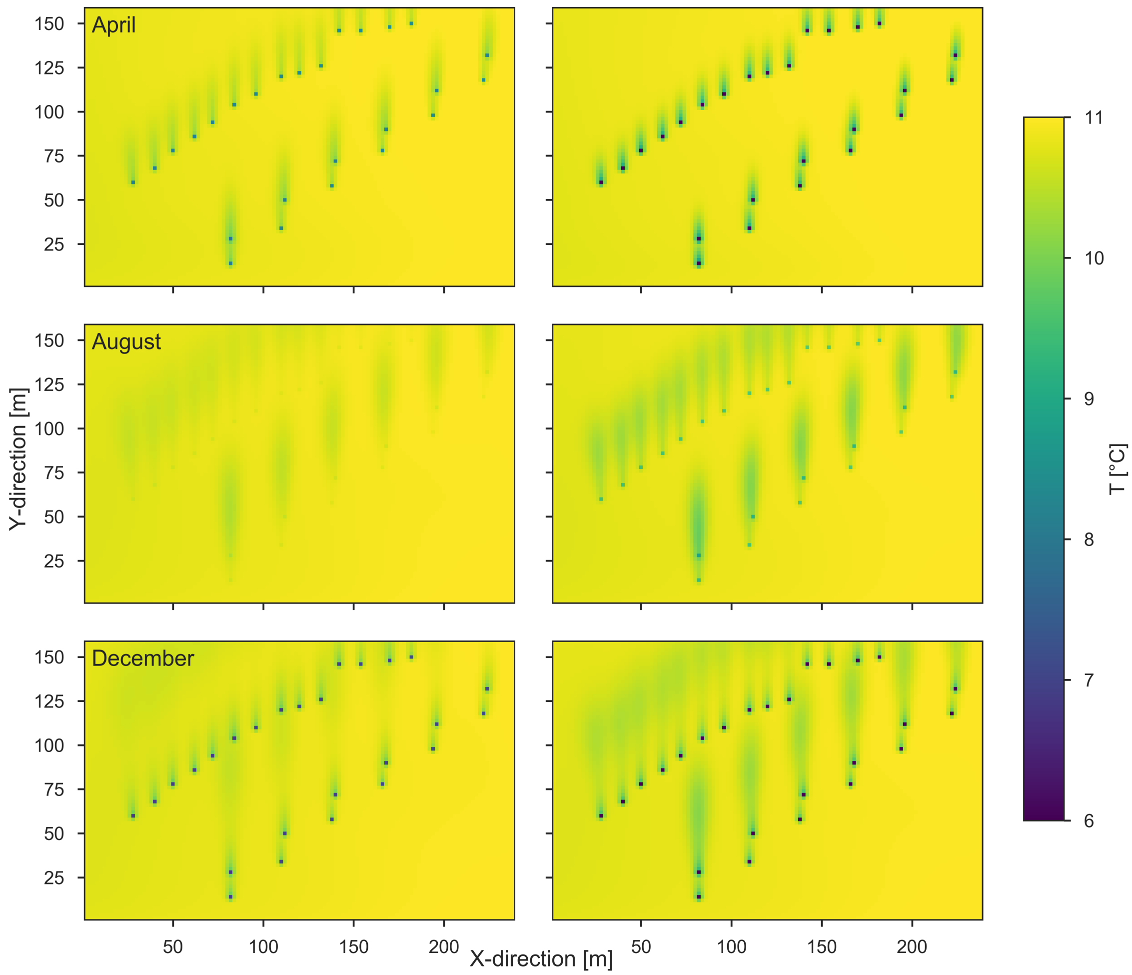

Figure 8: Map views of temperature slices at 50 m depth below surface. Left: Temperature slices for the BHE field assuming renovated buildings. Right: Temperature slices assuming original building structure.

bouring borehole heat exchangers in the model peak around day 180 in our simulations, which translates to end of June. Figure 9 shows a north-south temperature profile at 50 m below ground level at day 180. Undisturbed simulated temperatures at that depth are around 10.9 °C. Pronounced peaks in temperatures mark fluid temperatures in a borehole heat exchanger. Between the two BHEs in the south, temperatures are lower than the undisturbed temperatures, marking the influence of a thermal plume. The signal of the plume extends from the most southern BHE until around 80 m along the profile. The temperature difference between the two borehole heat exchangers is relatively small with around 0.3 °C. In the scenario with buildings in original conditions, temperature differences are significantly larger. Here, the plume of the most southern BHE causes a drop in temperature of about 1 °C. This in turn affects the thermal energy rate which can be provided by a borehole heat exhcanger installation. A slight decrease in temperature at around 100 m in both scenarios is thermal signal of a BHE adjacent to the profile. By offsetting the southern BHEs in an EW direction, the performance of BHEs in the southern part of the western model improves slightly, as thermal plumes do not directly cross neighbouring installations. Seasonal changes in heating power demand are reflected by northward migrating thermal plumes. If heating power demand decreases is equal to zero (as in

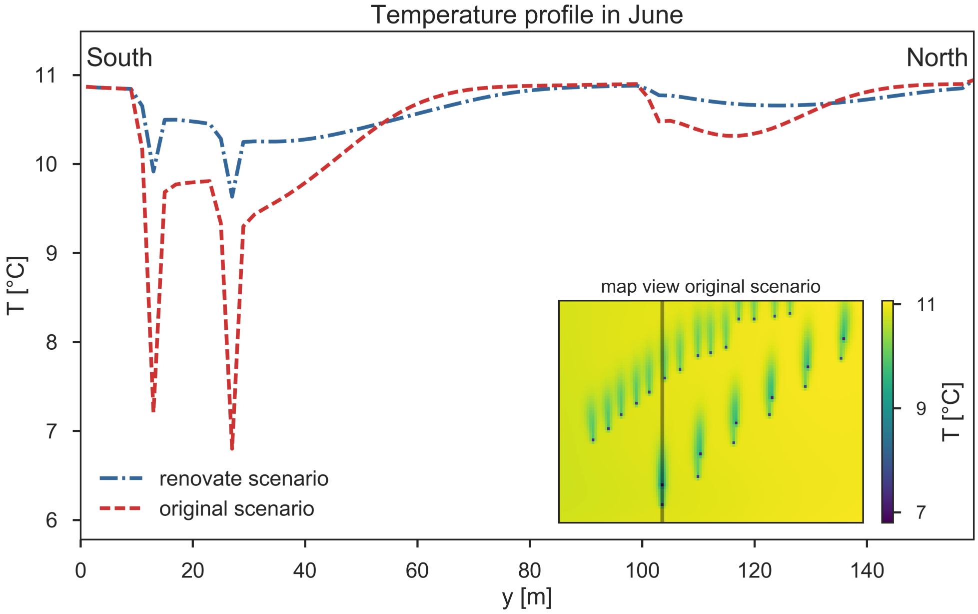

Figure 9: North South trending temperature profile at day 180 at a depth of 50 m below surface. Pronounced peaks are temperatures within the borehole heat exchangers. In between the peaks, temperatures are lower than the undisturbed temperature of 11 °C. The black line in the temperature field on the right shows the position of the temperature profile.

July/August in our simulation), temperatures in borehole heat exchangers re-equilibrates with surrounding temperatures. Thus thermal plumes of decreased temperatures caused by higher heating power demand end once heating power demand decreases, gets zero or negative (which equals cooling buildings).

6.2 Eastern model simulation

Such seasonal variations can be well observed in the eastern model. Figure 10 shows quaterly map views of temperature in the eastern model at a depth of 50 m. High hating power demand in the first four months yields thermal plumes of decreased temperatures. The extent of these plumes grows with continuous heating power demand (Fig. 10 June). If the demand equals zero over a longer time frame, temperatures arounde BHEs increase again, confining the plume of decreased temperatures. This plume is transported northward and exits the model domain via the northern lateral boundary (Fig. 10 September). This cycle repeats annualy, as it correlates with seasonal temperature changes via heating power demand. As stated before, visible thermal plumes are just observed in more permeable units, namely Hauptkies Aquifer and Quaternary Aquifer. Maximum simulated groundwater velocities in these aquifers are in the range of $70\,\mathrm{m\,a^{-1}}$. In deeper lithological units, such as the Inden and Ville Layers, no thermal plumes are observed and the heat transport towards BHE installations is dominated by conduction.

Different building scenarios exist for the eastern model, e.g. six single buildings (Fig. 3 right) or twelve semidetached houses. The latter would cover approximately the same area as six single houses. Accordingly, our simulation results can be evaluated for both scenarios, as the heating power demand is a function of net area, or number of floors. Those parameters do not vary significantly betweeen the two scenarios.

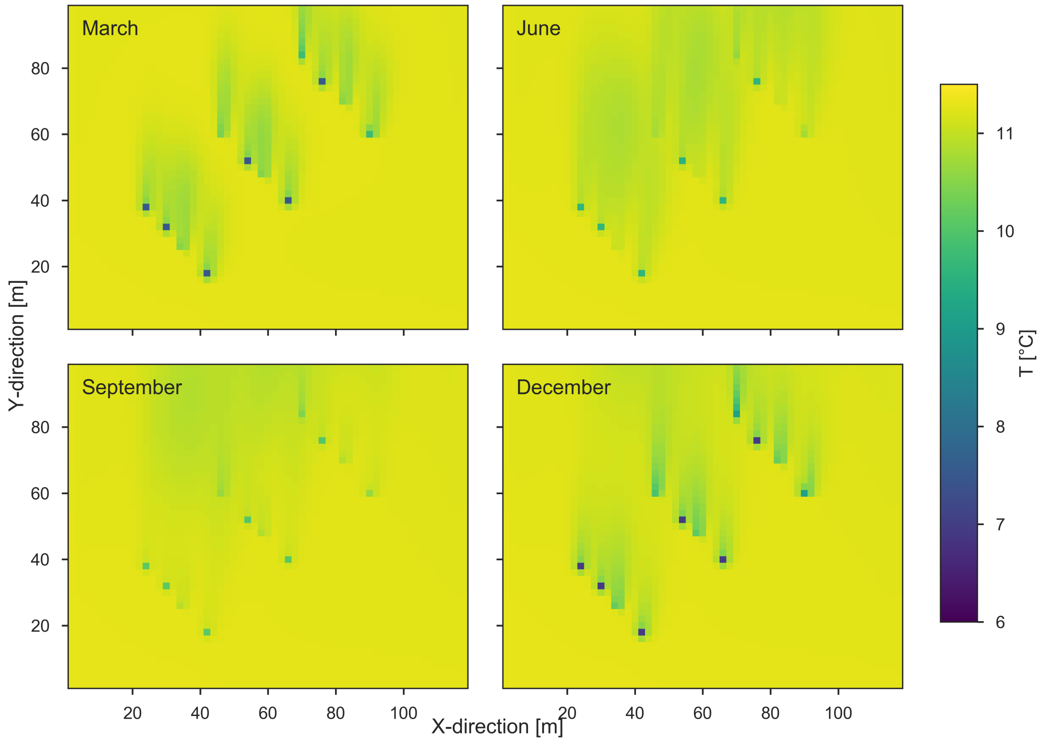

Figure 10: Map view of hydraulic potential in the western model (left) and the eastern model (right). Values of hydraulic head at lateral boundaries are kept constant and work as boundary conditions.

6.3 Transient temperature change along a BHE

In order to assess the annual temperature variations in a borehole heat exchanger, we plot the annual temperature spread along BHE length and variations of temperature with time exemplarily for one borehole heat exchanger (red circle in Figure 3). The average annual temperature spread within the BHE is around 4 °C (Fig. 11 left). Maximum temperatures (around 10.5 °C) correlate to initial conditions and phases of low heating power demand, thus the summer period. In turn, minimal temperatures (on average around 6.5 °C) correlate with high heating power demand during winter. At a depth of 60 m to 70 m, we see a distinct zone of decreased temperatures. In this depth, the borehole heat exchanger crosses the seam Schophoven, a lignite seam. One conclusion of Deliverable 4.2 was that lignite seams in the study area have a strong impact on the hydrothermal simulations and thus need to be resolved as realistic as possible. This conclusion is supported by temperature profiles along BHEs. Low permeability and low thermal conductivity of lignite seams inhibit heat transport towards the borehole heat exchanger. As a result, temperatures at depth, where lignite encompasses the borehole heat exchanger, are significantly lower than BHE-temperatures above or below the lignite seam. It should be noted that the significance of this effect is caused by the BHE-field implementation in SHEMAT-Suite. As previously stated, a BHE is implemented as a heat source- or sink term, depending on the thermal power demand, i.e. a Neumann boundary condition. Accordingly, temperatures in cells defined as a BHE are calculated to satisfy the boundary condition, thus temperatures decrease with continuous high thermal power demand. Due to the low thermal conductivity of lignite, heat transport towards the BHE is relatively inefficient, causing significantly lower temperatures in BHE-cells encompassed by lignite.

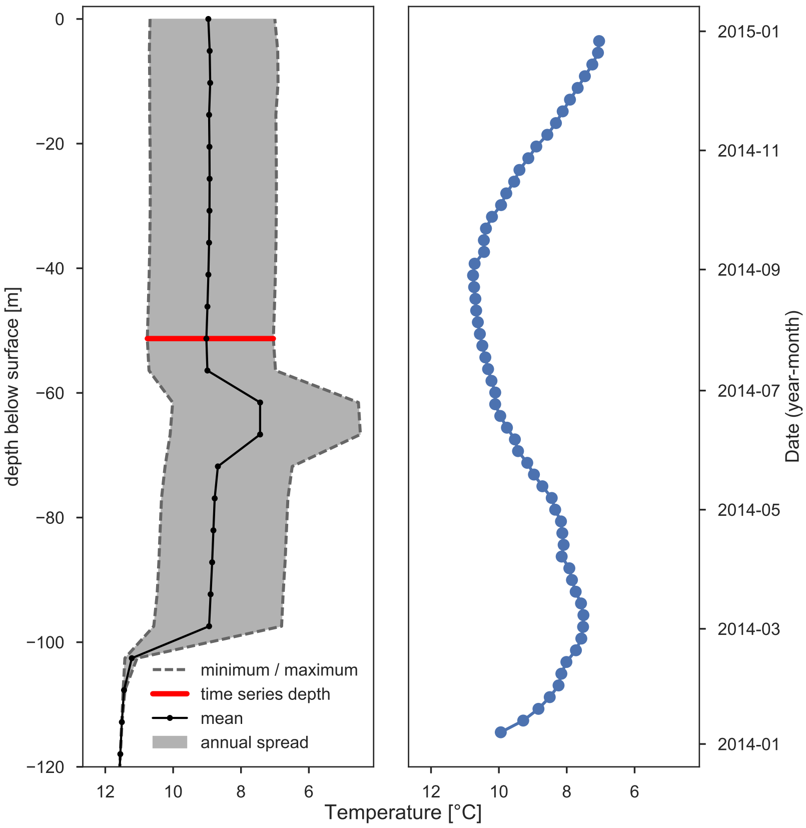

Figure 11: Visible insulating effect of the lignite seam at a depth of around 60 m in the subsurface. Potentially need to resolve this in vertical dimension!

Temperatures in those cells remain lower than neighbouring BHE cells, as flow within a BHE is not modelled in this approach (in contrast to the explicite BHE model). In reality, the effect of a lignite seam with low thermal conductivity would be considerably less pronounced due to flow in the BHE. The temperature development with time is assessed at a depth of 50 m below surface (red line in Fig. 11). As initial undisturbed temperatures are around 10 °C, a strong decrease in temperatures can be observed in the first two months. From March onwards, temperatures increase gradually until September, when temperatures in the BHE peak. Due to increase in heating power demand, temperatures decrease until simulation end. While this transient evolution suggests that a sustainable operation can be possible, a longer timeframe needs to be simulated for assessing a possible and sustainable BHE-field operation.

6.4 Western model simulation over 15 years

Simulations over a timeframe of 1 year do not suffice for estimating the sustainability of a BHE-field. Mottaghy & Dijkshoorn (2012) simulate a BHE-field for 15 years of operation in order to analyse sustainable operation of the simulated BHE-field. Further, using geothermal heat supply just for space heating will cool the subsurface over a longer timeframe. In order to evaluate the sustainability of the BHE-field, we extended the simulation time to 15 years for the western model, assuming refitted buildings. Figure 12 shows map views of temperature at a depth of 50 m below surface at summer of each year. Lower temperatures transported along groundwater flow yield thermal plumes

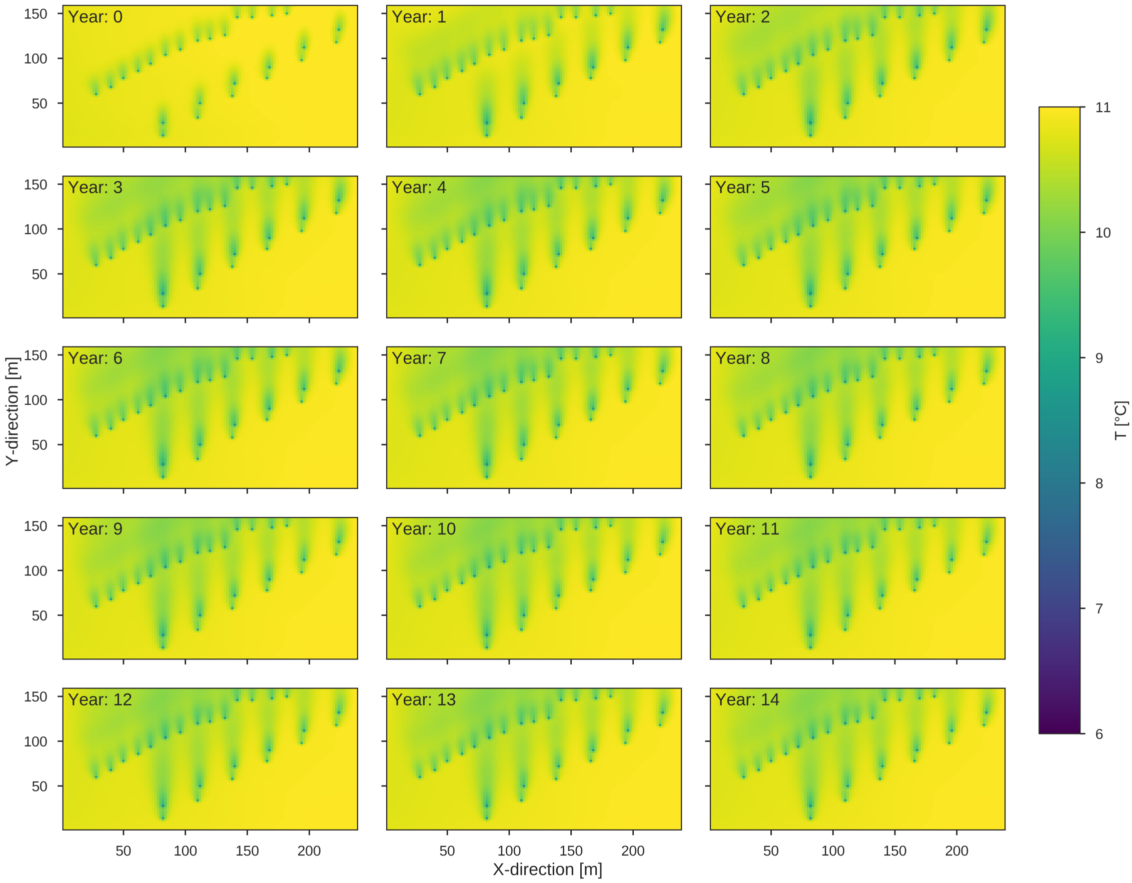

Figure 12: Map views of temperature in summer of each year.

similarly to the 1-year simulations. The effect of these thermal plumes increases with time due to continuous BHE operation. For assessing the magnitude of cooling in more detail, we plot, similarly to Figure 9, the temperature profile in june for each year. Temperatures along the profile significantly decrease from higher initial conditions over the first three years, due to the effect of groundwater velocity. However, temperatures stabilize at around 10 °C for the rest of the simulation. Accordingly, impact of thermal plumes also stabilizes. It should be noted, that the temperature curves underlying the heating power demand for the BHE-field do not comprise extreme events, such as long cold spells during winter. Instead, we assume a more regular, sinusoidal seasonal temperature pattern. Accordingly, temperatures stabilize at certain values, due to repeating boundary condition values, i.e. seasonal repeating heating power demands. However, a stabilization of temperatures under the assumed conditions suggests, that the simulated BHE-field could be operated sustainably. In our simulations, we just assumed heating power, not cooling during summer. Incorporating cooling would likely improve the BHE-field performance. A combination of heating and cooling, where surplus heat gets stored in the subsurface during summer, most likely increases a sustainable operation of a BHE-field.

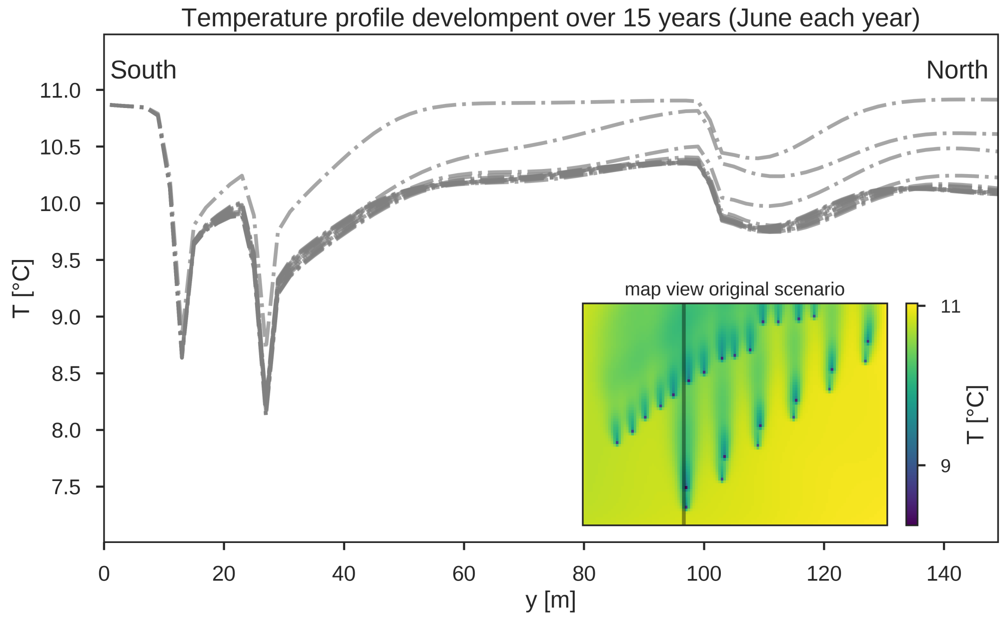

Figure 13: North South trending temperature profile for each year over a total simulation time of 15 years. Small subplot shows the location of the temperature profile.

7. Conclusions

Based on results of Deliverable 4.2, we generated two representative models for simulating the operation of borehole heat exchangers. In a western model, we compare BHE responses to thermal power demand in two scenarios: an original scenario, where buildings are assumed to remain in original conditions, and a renovated scenario, where buildings are assumed to be refitted to current energy standards. We simulate permanent BHE operation over a timeframe of one year. Simulation results suggest that the thermal power demand of refitted buildings can likely be met by borehole heat exchangers. Temperatures within a modelled BHE decrease to around 6 °C in winter due to high thermal power demand, and rise to around 10 °C in late summer. Simulations further show that groundwater flow should be considered in layout of BHE-fields, as high permeability in the Hauptkies Aquifer and Quaternary Aquifer enable northward groundwater velocities of up to $70\,\mathrm{m\,a^{-1}}$. Groundwater flow causes the development of thermal plumes, emanating from the borehole heat exchangers. Thermal plumes are transported by advective heat transport and increase thermal interaction between BHEs. However, simulation results suggest that this thermal interaction is relatively small and does not decrease the capacity of BHE installations affected by thermal plumes of neighbouring BHEs.

Prolonged simulations over a timeframe of 15 years yield stabilized temperatures around 1 °C below initial conditions at a depth of 50 m below surface. Temperatures around single BHE-units suggest that a sustainable operation of the simulated BHE-field is possible for a longer time. Sustainable operation can be improved by couplint heating and cooling of buildings, and using the subsurface as heat storage, i.e. store heat during cooling in summer and use this heat in winter.

References

Bode, G., Fütterer, J., & Müller, D., 2018. Mode and storage load based control of a complex building system with a geothermal field, *Energy and Buildings*, **158**, 1337 – 1345.

Clauser, C., 2003. *Numerical Simulation of Reactive Flow in Hot Aquifers: SHEMAT and Processing SHEMAT.*, Springer.

Erftverband, 2015. Grundwassergleichen stand 9. oktober 2015, `http://www.erftverband.de/grundwasserstand/`, accessed 2017.06.12.

Geilenkirchen, C., 2018. Ergebnisszenario v, `http://bift-gk.de/wp-content/uploads/2017/12/Staedtebauliches_Entwicklungszenario_V_Empfehlung_-1.pdf`, accessed 2018.02.24.

Hellström, G., 1991. *Ground heat storage: thermal analyses of duct storage systems*, Department of Mathematical Physics, Lund Univ.

Mottaghy, D. & Dijkshoorn, L., 2012. Implementing an effective finite difference formulation for borehole heat exchangers into a heat and mass transport code, *Renewable Energy*, **45**, 59 – 71.

Rath, V., Wolf, A., & Bücker, H., 2006. Joint three-dimensional inversion of coupled groundwater flow and heat transfer based on automatic differentiation: sensitivity calculation, verification, and synthetic examples, *Geophysical Journal International*, **167**(1), 453–466.

Remmen, P., Lauster, M., Mans, M., Fuchs, M., Osterhage, T., & Müller, D., 2018. Teaser: an open tool for urban energy modelling of building stocks, *Journal of Building Performance Simulation*, **11**(1), 84–98.